Eur. Phys. J. B **18**, 645–654 (2000)

THE EUROPEAN PHYSICAL JOURNAL B

EDP Sciences

Calculation of second topological moment $\langle m^2 \rangle$ of two entangled polymers

F. Ferrari[1,2], H. Kleinert[3,a], and I. Lazzizzera[1,2]

[1] Dipartimento di Fisica, Università di Trento, 38050 Povo, Italy
[2] INFN, Gruppo Collegato di Trento, 38050 Povo, Italy
[3] Institut für Theoretische Physik, Freie Universität Berlin, Arnimallee 14, 14195 Berlin, Germany

Received 22 March 2000 and Received in final form 22 September 2000

Abstract. We set up a field theoretical model based on Abelian Chern-Simons field theories to describe the topological entanglement of two polymers. The topological states of the system are distinguished using the link invariant of Gauss. The second topological moment of the two polymers $\langle m^2 \rangle$, where m is the linking number, is exactly computed by field theoretical methods. The result is applied to estimate approximatively the mean square average of the linking number of a polymer P_1 in a dilute solution with other polymers.

PACS. 61.41.+e Polymers, elastomers, and plastics – 05.40.-a Fluctuation phenomena, random processes, noise, and Brownian motion – 11.15.-q Gauge field theories

1 The problem

Consider two polymers P_1 and P_2 which statistically can be linked with each other any number of times $m = 0, 1, 2, \ldots$ The situation is illustrated in Figure 1 for $m = 2$.

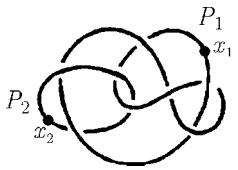

Fig. 1. Closed polymers P_1, P_2 with trajectories C_1, C_2 respectively.

We would like to find the probability distribution of the linking numbers m as a function of the lengths of P_1 and P_2. As a first contribution to solving this problem, we calculate the second moment of this distribution, $\langle m^2 \rangle$. The topological states of the two polymers will be distinguished here by means of the Gauss linking number, which counts how many times one polymer winds up around the other. Despite its incompleteness in the description of real polymers already noted in [1], the Gauss linking number is in general used in polymer physics because it is the simplest invariant that explicitly contains the polymer conformations, in contrast to algebraic invariants in knot theory [2].

[a] e-mail: kleinert@physik.fu-berlin.de

Even if the topological constraints are imposed using the Gauss link invariant, the analytical treatment of the two-polymer system is mathematically complex. Until now, only the fluctuations of one polymer, let us say P_1, could be treated exactly, while the fluctuations of P_2 have been taken into account using various approximations [3–6]. In [3], for instance, it has been assumed that P_2 is of fixed configuration. In this case, different configurations give different dependences of $\langle m^2 \rangle$ on the polymer lengths [3]. In [5], instead, the density of bond vectors of P_2 has been considered as Gaussian random variables. The second topological moment has then been computed in a non-field theoretical way using a pre-averaging approximation discussed in [7]. Other analytical approaches to the problem of topological entanglement of polymers, which are however not strictly related to the computation of the second topological moment, have been reviewed in [8–10]. In [11], for example, a set of relevant collective variables has been constructed in order to describe the fluctuations of a polymer P_1 linked to other polymers in a melt. If the total number of polymers is large, the statistical properties of these variables can be approximated by Gaussian statistics. Interesting results using this method have been obtained in [12], where the distribution function for the distance between segments located on different DNA rings has been computed for several linking numbers.

In the present work we follow a different strategy. The two-polymer problem is mapped into a field theory and the topological interactions, which enforce the Gaussian constraints on the polymers, are propagated by multicomponent Abelian Chern-Simons fields. In this way several simplifications occur and, in the absence of excluded

volume interactions, the computation of the second topological moment requires just the evaluation of four Feynman diagrams. Moreover, no approximation is necessary, so that the final result does not depend on the choice of the fixed obstacles or on the source of Gaussian noise.

As an application, we compute the mean-square winding number of a polymer in solution with others. In doing that, we follow the spirit of reference [13], where it was emphasized the importance of the two-polymer system as an useful approximation in treating an arbitrary number of polymers subjected to topological constraints. Focusing attention upon a particular molecule, P_1, the approximation consists in replacing all others by a single long effective molecule P_2.

Let $G_m(\mathbf{x}_1, \mathbf{x}_2; L_1, L_2)$ be the configurational probability to find the polymer P_1 of length L_1 with fixed coinciding end points at $\mathbf{x}_1$ and the polymer P_2 of length L_2 with fixed coinciding end points at $\mathbf{x}_2$, entangled with a Gaussian linking number m.

The second moment $\langle m^2 \rangle$ is defined by the ratio of integrals [3]

$$\langle m^2 \rangle = \frac{\int \mathrm{d}^3x_1 \mathrm{d}^3x_2 \int_{-\infty}^{+\infty} \mathrm{d}m \; m^2 G_m\left(\mathbf{x}_1, \mathbf{x}_2; L_1, L_2\right)}{\int \mathrm{d}^3x_1 \mathrm{d}^3x_2 \int_{-\infty}^{+\infty} \mathrm{d}m \, G_m\left(\mathbf{x}_1, \mathbf{x}_2; L_1, L_2\right)} \quad (1)$$

performed for either of the two probabilities. The integrations in $\mathrm{d}^3x_1\mathrm{d}^3x_2$ covers all positions of the end points. The denominator plays the role of a partition function of the system:

$$Z \equiv \int \mathrm{d}^3x_1 \mathrm{d}^3x_2 \int_{-\infty}^{+\infty} \mathrm{d}m \, G_m\left(\mathbf{x}_1, \mathbf{x}_2; L_1, L_2\right). \quad (2)$$

Due to translational invariance of the system, the probabilities depend only on the differences between the end point coordinates:

$$G_m\left(\mathbf{x}_1, \mathbf{x}_2; L_1, L_2\right) = G_m\left(\mathbf{x}_1 - \mathbf{x}_2; L_1, L_2\right). \quad (3)$$

Thus, after the shift of variables, the spatial double integrals in (1) can be rewritten as

$$\int \mathrm{d}^3x_1 \mathrm{d}^3x_2 G_m(\mathbf{x}_1 - \mathbf{x}_2; L_1, L_2) = V \int \mathrm{d}^3x \, G_m(\mathbf{x}; L_1, L_2), \quad (4)$$

where V denotes the total volume of the system.

2 Polymer field theory for probabilities

The linking number for the two polymers is given by the Gauss integral

$$I_G(P_1, P_2) = \frac{1}{4\pi} \oint_{P_1} \oint_{P_2} [\mathrm{d}\mathbf{x}_1 \times \mathrm{d}\mathbf{x}_2] \cdot \frac{\mathbf{x}_1 - \mathbf{x}_2}{|\mathbf{x}_1 - \mathbf{x}_2|^3}. \quad (5)$$

It takes the values $m = 0, \pm 1, \pm 2, \ldots$ With the help of two vector potentials $\mathbf{A}_1$ and $\mathbf{A}_2$, the phase factor $\mathrm{e}^{\mathrm{i}m\lambda}$ can be obtained as a result of a local gauge theory of the Abelian Chern-Simons type:

$$\mathrm{e}^{\mathrm{i}m\lambda} = \int \mathcal{D}A_1^\mu \mathcal{D}A_2^\mu \times \mathrm{e}^{-\mathcal{A}_{\mathrm{CS}} - \int_{P_1} \mathrm{d}\mathbf{x}_1 \cdot \mathbf{A}_1 - \lambda \int_{P_2} \mathrm{d}\mathbf{x}_2 \cdot \mathbf{A}_2}, \quad (6)$$

where $\mathcal{A}_{\mathrm{CS}}$ is the action

$$\mathcal{A}_{\mathrm{CS}} = \mathrm{i}\kappa \int \mathrm{d}^3x \, \varepsilon_{\mu\nu\rho} A_1^\mu \partial_\nu A_2^\rho, \quad (7)$$

Indeed, the correlation functions $D_{ij}^{\mu\nu}(\mathbf{x}, \mathbf{x}')$ of the gauge fields

$$\langle A_1^\mu(\mathbf{x}) A_1^\nu(\mathbf{x}') \rangle = 0, \quad \langle A_2^\mu(\mathbf{x}) A_2^\nu(\mathbf{x}') \rangle = 0, \quad (8)$$

$$\langle A_1^\mu(\mathbf{x}) A_2^\nu(\mathbf{x}') \rangle = \int \frac{\mathrm{d}^3p}{(2\pi)^3} \mathrm{e}^{\mathrm{i}\mathbf{p}(\mathbf{x}-\mathbf{x}')} \frac{\mathrm{i}\epsilon_{\mu\lambda\nu} p^\lambda}{\mathbf{p}^2} \quad (9)$$

$$= \frac{1}{4\pi} \epsilon_{\mu\lambda\nu} \nabla_\lambda \frac{1}{|\mathbf{x} - \mathbf{x}'|}$$

$$= \frac{1}{4\pi} \epsilon_{\mu\nu\kappa} \frac{(x - x')^\lambda}{|\mathbf{x} - \mathbf{x}'|^3}, \quad (10)$$

are such that the functional integral on the right-hand side of (6) produces directly the phase factor $\mathrm{e}^{\mathrm{i}I_G(P_1,P_2)\lambda}$ with the eigenvalue $\mathrm{e}^{\mathrm{i}m\lambda}$. We can select configurations with a certain value of m from all configurations by forming the integral $\int_{-\infty}^{\infty} \mathrm{d}\lambda \mathrm{e}^{-\mathrm{i}m\lambda}$ over this quantity. At this point, it is convenient to define an auxiliary probability $G_\lambda(\overrightarrow{\mathbf{x}_1}, \overrightarrow{\mathbf{x}_2}; \overrightarrow{z})$, which is the Fourier transformed of the original configurational probability with respect to m. This function measures the probability to find the polymer P_1 with open ends at $\mathbf{x}_1, \mathbf{x}_1'$ and the polymer P_2 with open ends at $\mathbf{x}_2, \mathbf{x}_2'$, while the chemical potential conjugated to the topological number m is given by λ. The double vectors $\overrightarrow{\mathbf{x}_1} \equiv (\mathbf{x}_1, \mathbf{x}_1')$ and $\overrightarrow{\mathbf{x}_2} \equiv (\mathbf{x}_2, \mathbf{x}_2')$ collect initial and final endpoints of the two polymers P_1 and P_2. Here we follow the approach of Edwards [1], in which one starts with open polymers with fixed ends. The case of closed polymers, where m becomes a true topological number and it is thus relevant in the present context, is recovered in the limit of coinciding extrema. We notice that in this way one introduces in the configurational probability an artificial dependence on the fixed points $\mathbf{x}_1$ and $\mathbf{x}_2$. In physical situations, however, the fluctuations of the polymers are entirely free. For this reason, we have averaged in (1) over all possible fixed points by means of the integrations in $\mathrm{d}^3\mathbf{x}_1\mathrm{d}^3\mathbf{x}_2$.

The most efficient way of describing the statistical fluctuations of the polymers P_1 and P_2 is by introducing two complex polymer fields $\psi_1^{a_1}(\mathbf{x}_1)$ and $\psi_2^{a_2}(\mathbf{x}_2)$ with n_1 and n_2 replica ($a_1 = 1, \ldots, n_1$, $a_2 = 1, \ldots, n_2$). At the end we shall take $n_1, n_2 \to 0$ to ensure that these fields describe only one polymer each [10]. The auxiliary probability $G_\lambda(\overrightarrow{\mathbf{x}_1}, \overrightarrow{\mathbf{x}_2}; \overrightarrow{z})$ can be expressed as a functional integral [14] over the replica fiends and the topological fields as follows

$$G_\lambda(\overrightarrow{\mathbf{x}_1}, \overrightarrow{\mathbf{x}_2}; \overrightarrow{z}) = \lim_{n_1, n_2 \to 0} \int \mathcal{D}(\text{fields}) \times \psi_1^{a_i}(\mathbf{x}_1) \psi_1^{*a_1}(\mathbf{x}_1') \psi_2^{a_2}(\mathbf{x}_2) \psi_2^{*a_2}(\mathbf{x}_2') \mathrm{e}^{-\mathcal{A}}, \quad (11)$$

where $\mathcal{D}$(fields) indicates the measure of functional integration and $\mathcal{A}$ the action governing the fluctuations. The expectation value is calculated for any fixed pair (a_1, a_2) of replica labels, *i.e.*, replica labels are not subject to Einstein's summation convention of repeated indices. The action $\mathcal{A}$ consists of kinetic terms for the fields, a quartic interaction of the fields to account for the fact that two monomers of the polymers cannot occupy the same point, the so-called *excluded-volume effect*, and a Abelian Chern-Simons field to describe the linking number m [14]. Neglecting at first the excluded-volume effect and focusing attention on the linking problem only, the action reads

$$\mathcal{A} = \mathcal{A}_{\rm CS} + \mathcal{A}_{\rm pol}, \tag{12}$$

with a polymer field action

$$\mathcal{A}_{\rm pol} = \sum_{i=1}^{2} \int \mathrm{d}^3\mathbf{x} \left[|\bar{\mathbf{D}}^i \Psi_i|^2 + m_i^2 |\Psi_i|^2 \right]. \tag{13}$$

Here we have omitted a gauge fixing term, which enforces the Lorentz gauge. The topological vector fields are coupled to the polymer fields by the covariant derivatives

$$\mathbf{D}^i = \boldsymbol{\nabla} + \mathrm{i}\gamma_i \mathbf{A}_i, \tag{14}$$

with the coupling constants $\gamma_{1,2}$ given by

$$\gamma_1 = \kappa \qquad \gamma_2 = \lambda. \tag{15}$$

The square masses of the polymer fields are

$$m_i^2 = 2Mz_i, \tag{16}$$

where $M = 3/a$ and a represents the length of the polymer links. z_1 and z_2 are chemical potentials, measured in units of the temperature, conjugated to the length parameters L_1 and L_2 respectively. To make closer the analogy with the usual field theories, we have introduced the pseudo-constant of Planck $\hbar = Ma/3$ and the mass parameter M has been fixed by requiring that $\hbar = 1$.

The symbols Ψ_i collect the replicas of the two polymer fields

$$\Psi_i = \left(\psi_i^1, \ldots, \psi_i^{n_i}\right), \tag{17}$$

and their absolute squares contain the sums over all the replicas

$$|\mathbf{D}^i \bar{\Psi}_i|^2 = \sum_{a_i=1}^{n_i} |\mathbf{D}^i \psi_i^{a_i}|^2, \quad |\Psi_i|^2 = \sum_{a_i=1}^{n_i} |\psi_i^{a_i}|^2. \tag{18}$$

Having specified the fields, we can now write down the measure of functional integration in equation (11):

$$\mathcal{D}(\text{fields}) = \int \mathcal{D}A_1^\mu \mathcal{D}A_2^\nu \mathcal{D}\Psi_1 \mathcal{D}\Psi_1^* \mathcal{D}\Psi_2 \mathcal{D}\Psi_2^*. \tag{19}$$

By equation (6), the parameter λ is conjugate to the linking number m. We can therefore calculate the probability $G_m(\overrightarrow{\mathbf{x}_1}, \overrightarrow{\mathbf{x}_2}; L_1, L_2)$ in which the two polymers are open with different endpoints from the auxiliary one $G_\lambda(\overrightarrow{\mathbf{x}_1}, \overrightarrow{\mathbf{x}_2}; \overrightarrow{z})$ by the following Laplace integral over $\overrightarrow{z} = (z_1, z_1)$:

$$G_m(\overrightarrow{\mathbf{x}_1}, \overrightarrow{\mathbf{x}_2}; L_1, L_2) = \lim_{\substack{\mathbf{x}_1' \to \mathbf{x}_1 \\ \mathbf{x}_2' \to \mathbf{x}_2}} \int_{c-\mathrm{i}\infty}^{c+\mathrm{i}\infty} \frac{M\mathrm{d}z_1}{2\pi\mathrm{i}} \frac{M\mathrm{d}z_2}{2\pi\mathrm{i}} \mathrm{e}^{z_1 L_1 + z_2 L_2} \times \int_{-\infty}^{\infty} \mathrm{d}\lambda \mathrm{e}^{-\mathrm{i}m\lambda} G_\lambda\left(\overrightarrow{\mathbf{x}_1}, \overrightarrow{\mathbf{x}_2}; \overrightarrow{z}\right). \tag{20}$$

In the above formula c denotes as usual a vertical contour in the complex plane chosen so that all singularities of the integrand are to the left of it.

3 Calculation of the second topological moment

At this point the calculation of the second topological moment (1) can be performed starting from the configurational probability given in equation (20) and using pure field theoretical techniques.

Let us start with the partition function (2). By equation (20), it is given by the integral over the auxiliary probabilities

$$Z = \int \mathrm{d}^3x_1 \mathrm{d}^3x_2 \lim_{\substack{\mathbf{x}_1' \to \mathbf{x}_1 \\ \mathbf{x}_2' \to \mathbf{x}_2}} \int_{c-\mathrm{i}\infty}^{c+\mathrm{i}\infty} \frac{M\mathrm{d}z_1}{2\pi\mathrm{i}} \frac{M\mathrm{d}z_2}{2\pi\mathrm{i}} \mathrm{e}^{z_1 L_1 + z_2 L_2} \times \int_{-\infty}^{+\infty} \mathrm{d}m \int_{-\infty}^{+\infty} \mathrm{d}\lambda \mathrm{e}^{-\mathrm{i}m\lambda} G_\lambda\left(\overrightarrow{\mathbf{x}_1}, \overrightarrow{\mathbf{x}_2}; \overrightarrow{z}\right). \tag{21}$$

The integration over m is trivial and gives $2\pi\delta(\lambda)$, enforcing $\lambda = 0$, so that

$$Z = \int \mathrm{d}^3x_1 \mathrm{d}^3x_2 \lim_{\substack{\mathbf{x}_1' \to \mathbf{x}_1 \\ \mathbf{x}_2' \to \mathbf{x}_2}} \int_{c-\mathrm{i}\infty}^{c+\mathrm{i}\infty} \frac{M\mathrm{d}z_1}{2\pi\mathrm{i}} \frac{M\mathrm{d}z_2}{2\pi\mathrm{i}} \mathrm{e}^{z_1 L_1 + z_2 L_2} \times G_{\lambda=0}\left(\overrightarrow{\mathbf{x}_1}, \overrightarrow{\mathbf{x}_2}; \overrightarrow{z}\right). \tag{22}$$

To compute $G_{\lambda=0}\left(\overrightarrow{\mathbf{x}_1}, \overrightarrow{\mathbf{x}_2}; \overrightarrow{z}\right)$ we observe that the action $\mathcal{A}$ in equation (12) is quadratic in λ. Let us expand $\mathcal{A}$ as

$$\mathcal{A} = \mathcal{A}_0 + \lambda \mathcal{A}_1 + \lambda^2 \mathcal{A}_2 \tag{23}$$

with the λ-independent part

$$\mathcal{A}_0 \equiv \mathcal{A}_{\rm CS} + \int \mathrm{d}^3x \left[|\mathbf{D}_1 \Psi_1|^2 + |\boldsymbol{\nabla} \Psi_2|^2 + \sum_{i=1}^{2} m_i^2 |\Psi_i|^2 \right], \tag{24}$$

a linear coefficient

$$\mathcal{A}_1 \equiv \int \mathrm{d}^3x \; \mathbf{j}_2(\mathbf{x}) \cdot \mathbf{A}_2(\mathbf{x}) \tag{25}$$

containing a "current" of the second polymer field

$$\mathbf{j}_2(\mathbf{x}) = \mathrm{i}\Psi_2^*(\mathbf{x}) \boldsymbol{\nabla} \Psi_2(\mathbf{x}), \tag{26}$$

and a quadratic coefficient

$$\mathcal{A}_2 \equiv \frac{1}{4}\int \mathrm{d}^3\mathbf{x}\ \mathbf{A}_2^2|\Psi_2(\mathbf{x})|^2. \tag{27}$$

With these definitions we write with the help of (24):

$$G_{\lambda=0}\left(\overrightarrow{\mathbf{x}_1},\overrightarrow{\mathbf{x}_2};\overrightarrow{z}\right) = \int \mathcal{D}(\text{fields})\mathrm{e}^{-\mathcal{A}_0} \times\psi_1^{a_1}(\mathbf{x}_1)\psi_1^{*a_1}(\mathbf{x}_1')\psi_2^{a_2}(\mathbf{x}_2)\psi_2^{a_2}(\mathbf{x}'). \tag{28}$$

Let us now turn to the numerator in equation (1):

$$N \equiv \int \mathrm{d}^3x_1\mathrm{d}^3x_2\int_{-\infty}^{\infty}\mathrm{d}m\ m^2 G_m\left(\mathbf{x}_1,\mathbf{x}_2;L_1,L_2\right). \tag{29}$$

We shall set up a functional integral for N in terms of the auxiliary probability $G_\lambda\left(\overrightarrow{\mathbf{x}_1},\overrightarrow{\mathbf{x}_2};\overrightarrow{z}\right)$ analogous to equation (21). First we observe that

$$N = \int \mathrm{d}^3\mathbf{x}_1\mathrm{d}^3r_2\int_{-\infty}^{\infty}\mathrm{d}m\ m^2\lim_{\substack{\mathbf{x}_1'\to\mathbf{x}_1\\ \mathbf{x}_2'\to\mathbf{x}_2}}\int_{c-\mathrm{i}\infty}^{c+\mathrm{i}\infty}\frac{\mathrm{d}z_i}{2\pi\mathrm{i}}\frac{\mathrm{d}z_2}{2\pi\mathrm{i}} \times\mathrm{e}^{z_1L_1+z_2L_2}\int_{-\infty}^{\infty}\mathrm{d}\lambda\mathrm{e}^{-\mathrm{i}m\lambda}G_\lambda\left(\overrightarrow{\mathbf{x}_1},\overrightarrow{\mathbf{x}_2};\overrightarrow{z}\right). \tag{30}$$

The integration over m is easily performed after noting that

$$\int_{-\infty}^{\infty}\mathrm{d}m\ m^2\mathrm{e}^{-\mathrm{i}m\lambda}G_\lambda\left(\overrightarrow{\mathbf{x}_1},\overrightarrow{\mathbf{x}_2};\overrightarrow{z}\right) = -\int_{-\infty}^{\infty}\mathrm{d}m\left(\frac{\partial^2}{\partial\lambda^2}\mathrm{e}^{-\mathrm{i}m\lambda}\right)G_\lambda\left(\overrightarrow{\mathbf{x}_1},\overrightarrow{\mathbf{x}_2};\overrightarrow{z}\right). \tag{31}$$

After two integrations by parts in λ and an integration in m, we obtain

$$N = \int \mathrm{d}^3x_1\mathrm{d}^3x_2\lim_{\substack{\mathbf{x}_1'\to\mathbf{x}_1\\ \mathbf{x}_2'\to\mathbf{x}_2}}(-1)\int_{c-\mathrm{i}\infty}^{c+\mathrm{i}\infty}\frac{M\mathrm{d}z_1}{2\pi\mathrm{i}}\frac{M\mathrm{d}z_2}{2\pi\mathrm{i}}\mathrm{e}^{z_1L_1+z_2L_2} \times\int_{-\infty}^{\infty}\mathrm{d}\lambda\ \delta(\lambda)\left[\frac{\partial^2}{\partial\lambda^2}G_\lambda\left(\overrightarrow{\mathbf{x}_1},\overrightarrow{\mathbf{x}_2};\overrightarrow{z}\right)\right]. \tag{32}$$

The partial integrations in λ have been performed remembering that, because of equations (23, 27), $G_\lambda\left(\overrightarrow{\mathbf{x}_1},\overrightarrow{\mathbf{x}_2};\overrightarrow{z}\right)$ satisfies the following property:

$$\lim_{\lambda\to\pm\infty}G_\lambda\left(\overrightarrow{\mathbf{x}_1},\overrightarrow{\mathbf{x}_2};\overrightarrow{z}\right) = 0. \tag{33}$$

The now trivial integration in $\mathrm{d}\lambda$ yields

$$N = \int \mathrm{d}^3x_1\mathrm{d}^3x_2\lim_{\substack{\mathbf{x}_1'\to\mathbf{x}_1\\ \mathbf{x}_2'\to\mathbf{x}_2}}(-1)\int_{c-\mathrm{i}\infty}^{c+\mathrm{i}\infty}\frac{M\mathrm{d}z_1}{2\pi\mathrm{i}}\frac{M\mathrm{d}z_2}{2\pi\mathrm{i}}\mathrm{e}^{z_1L_1+z_2L_2} \times\left[\frac{\partial^2}{\partial\lambda^2}G_\lambda\left(\overrightarrow{\mathbf{x}_1},\overrightarrow{\mathbf{x}_2};\overrightarrow{z}\right)\right]_{\lambda=0}. \tag{34}$$

To compute the term in brackets, we use again (23) and equations (24–27), to find

$$N = \int \mathrm{d}^3x_1\mathrm{d}^3x_2\lim_{\substack{n_1\to0\\ n_2\to0}}\int_{c-\mathrm{i}\infty}^{c+\mathrm{i}\infty}\frac{M\mathrm{d}z_1}{2\pi\mathrm{i}}\frac{M\mathrm{d}z_2}{2\pi\mathrm{i}}\mathrm{e}^{z_1L_1+z_2L_2} \times\int\mathcal{D}(\text{fields})\ \exp(-\mathcal{A}_0)|\psi_1^{a_1}(\mathbf{x}_1)|^2|\psi_2^{a_2}(\mathbf{x}_2)|^2 \times\left[\left(\int\mathrm{d}^3x\ \mathbf{A}_2\cdot\Psi_2^*\boldsymbol{\nabla}\Psi_2\right)^2+\frac{1}{2}\int\mathrm{d}^3x\ \mathbf{A}_2^2\,|\Psi_2|^2\right]. \tag{35}$$

In this equation we have taken the limits of coinciding endpoint inside the Laplace integral over z_1, z_2. This will be justified later on the grounds that the potentially dangerous Feynman diagrams containing the insertions of operations like $|\Psi_i|^2$ vanish in the limit $n_1, n_2 \to 0$.

In order to calculate (35), we decompose the action into a free part

$$\mathcal{A}_0^0 \equiv \mathcal{A}_{\mathrm{CS}} + \int\mathrm{d}^3x\left[|\boldsymbol{\nabla}\Psi_1|^2+|\boldsymbol{\nabla}\Psi_2|^2+\sum_{i=1}^{2}m_i^2|\Psi_i|^2\right], \tag{36}$$

and interacting parts

$$\mathcal{A}_0^1 \equiv \int\mathrm{d}^3x\ \mathbf{j}_1(\mathbf{x})\cdot\mathbf{A}_1(\mathbf{x}) \tag{37}$$

with a "current" of the first polymer field

$$\mathbf{j}_1(\mathbf{x}) \equiv \mathrm{i}\Psi_1^*(\mathbf{x})\boldsymbol{\nabla}\Psi_1(\mathbf{x}), \tag{38}$$

and

$$\mathcal{A}_0^2 \equiv \frac{1}{4}\int\mathrm{d}^3\mathbf{x}\ \mathbf{A}_1^2|\Psi_1(\mathbf{x})|^2. \tag{39}$$

Expanding the exponential

$$\mathrm{e}^{-\mathcal{A}_0} = \mathrm{e}^{-(\mathcal{A}_0^0+\mathcal{A}_0^1+\mathcal{A}_0^2)} = \mathrm{e}^{-\mathcal{A}_0^0}\left[1-\mathcal{A}_0^1+\frac{(\mathcal{A}_0^1)^2}{2}-\mathcal{A}_0^2+\dots\right], \tag{40}$$

and keeping only the relevant terms, the functional integral (35) can be rewritten as a purely Gaussian expectation value

$$N = \kappa^2\int\mathrm{d}^3x_1\mathrm{d}^3x_2\lim_{\substack{n_1\to0\\ n_2\to0}}\int_{c-\mathrm{i}\infty}^{c+\mathrm{i}\infty}\frac{M\mathrm{d}z_1}{2\pi\mathrm{i}}\frac{M\mathrm{d}z_2}{2\pi\mathrm{i}}\mathrm{e}^{z_1L_1+z_2L_2} \times\int\mathcal{D}(\text{fields})\ \exp(-\mathcal{A}_0^0)|\psi_1^{a_1}(\mathbf{x}_1)|^2|\psi_2^{a_2}(\mathbf{x}_2)|^2 \times\left[\left(\int\mathrm{d}^3x\ \mathbf{A}_1\cdot\Psi_1^*\boldsymbol{\nabla}\Psi_1\right)^2+\frac{1}{2}\int\mathrm{d}^3x\ \mathbf{A}_1^2\,|\Psi_1|^2\right] \times\left[\left(\int\mathrm{d}^3x\ \mathbf{A}_2\cdot\Psi_2^*\boldsymbol{\nabla}\Psi_2\right)^2+\frac{1}{2}\int\mathrm{d}^3x\ \mathbf{A}_2^2\,|\Psi_2|^2\right]. \tag{41}$$

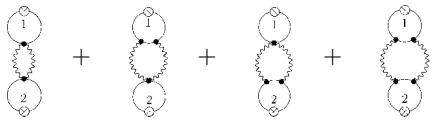

Fig. 2. The four diagrams contributing in equation (41). Full lines indicate correlation functions of Ψ_i-fields. The crossed circles with label i denote the insertion of $|\psi_i^{a_i}(\mathbf{x}_i)|^2$. Wavy lines represent the Chern-Simons vector fields.

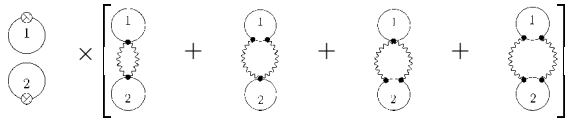

Fig. 3. Disconnected diagrams arising from equation (41) after Wick contractions. The conventions are the same of Figure 2. These diagrams vanish identically in the zero replica limit.

Only the four diagrams shown in Figure 2 contribute in equation (41).

Note that the initially asymmetric treatment of polymers P_1 and P_2 in the action (12) has led to a completely symmetric expression for the second moment.

Only the first diagram in Figure 2 is singular due to the divergence of the loop formed by two vector correlation functions. This infinity may be absorbed in the four-Ψ interaction accounting for the excluded volume effect which we do not consider at the moment. No divergence arises from the insertion of the composite fields $|\psi_i^{a_i}(\mathbf{x}_i)|^2$. In this respect, the disconnected diagrams shown in Figure 3 are potentally dangerous.

But these vanish in the limit of zero replica indices $n_1, n_2 \to 0$.

4 Regularization of the ultraviolet divergences

As we have seen in the previous section, the Feynman diagrams involved in the computation of $\langle m^2 \rangle$ are affected by ultraviolet (UV) divergences, which should be properly regularized. From a field theoretical point of view, this can be done in the frame of standard renormalization techniques. In the present case the situation is quite simple, because the number of relevant diagrams to be computed is finite. Actually, only the first graph in Figure 2 is divergent. The major difficulty is given by the presence of the completely antisymmetric tensor $\epsilon^{\mu\nu\rho}$ in the Chern-Simons action, which requires some care in order to avoid ambiguities [15]. Alternatively, it is possible to choose the Pauli-Villars regularization as for instance in [16].

Once a suitable regularization has been selected, one can start the renormalization program for the theory given in equation (13). To this purpose, we notice that to obtain non-vanishing Feynman diagrams, the same number of fields $\mathbf{A}_1$ and $\mathbf{A}_2$ should be contracted together. Moreover, the vertices propagating the topological interactions of the monomers with the fields $\mathbf{A}_2$ are proportional either to λ or to λ^2. Therefore, it is not difficult to realize that the counterterms which are needed to subtract the UV singularities are proportional to powers in λ of order $n \geq 1$. On the other side, from equations (22) and (35), it turns out that the second topological moment depends on the auxiliary probability $G_\lambda(\overrightarrow{\mathbf{x}_1}, \overrightarrow{\mathbf{x}_2}; \overrightarrow{z})$ and its derivatives up to the second degree evaluated at the point $\lambda = 0$. Thus, diagrams which contain six vertices or more are proportional to powers of λ of order three or higher and vanish in the limit $\lambda = 0$. As a consequence, for all practical purposes, only a finite number of Feynman diagrams and counterterms is necessary to compute $\langle m^2 \rangle$ exactly.

The problem of the above point of view is that UV divergences occur at infinitesimal distances, while in polymer physics it makes certainly no sense to consider phenomena at length-scales smaller than the monomer size. Indeed, in real polymers there is a minimal short-distance scale which provides a natural cut-off to UV singularities. In principle, one could choose the monomer size as a short-distance scale, but this would not be phenomenologically correct. In the approach of Edwards, in fact, the polymers are treated as random chains, but one should not forget that in the laboratory the monomers are usually not freely movable, so that polymers have a certain stiffness. This gives rise to a certain persistence length ξ_0 over which a polymer is stiff. Such length scale is increased to $\xi > \xi_0$ by the excluded-volume effects. ξ is the physical parameter which we are searching as a proper short-distance cut-off.

In this way, it is possible for instance to provide a simple regularization by cutting off all ultraviolet-divergent continuum integrals at distances smaller than ξ. This procedure is however somewhat euristhic, so that here we prefer to impose the cutoff in a rigorous way by imagining the model as being defined on a simple cubic lattice of spacing ξ. In this way, it arises of course the difficulty of computing space integrals on a lattice. This task can be achieved only numerically. Nevertheless, we will show that in the physical limit in which the polymers become very long, the discrete integrals may be replaced by continuous ones and it is possible to perform all calculations analytically. This has a physical explanation. Indeed, if the polymer lengths are much larger than the persistence length, the effects due to the finite monomer size become negligible and can be ignored.

5 Calculation of the partition function

We start the explicit calculation of Z by noting that in the action (24), the fields Ψ_2, Ψ_2^* are obviously free, whereas the fields Ψ_1, Ψ_1^* are apparently not because of the couplings with the Chern-Simons fields in the covariant derivative $\mathbf{D}^1$. This coupling is, however, without physical consequences: Indeed, by integrating out A_2^μ in (28), we find the flatness condition:

$$\boldsymbol{\nabla} \times \mathbf{A}_1 = 0. \tag{42}$$

On a flat space with vanishing boundary conditions at infinity this implies $\mathbf{A}_1 = 0$. As a consequence, the functional integral (28) factorizes

$$G_{\lambda=0}\left(\overrightarrow{\mathbf{x}_1}, \overrightarrow{\mathbf{x}_2}; \overrightarrow{z}\right) = G_0(\mathbf{x}_1 - \mathbf{x}'_1; z_1) G_0(\mathbf{x}_2 - \mathbf{x}'_2; z_2), \tag{43}$$

where $G_0(\mathbf{x}_i - \mathbf{x}'_i; z_i)$ are the free correlation functions of the polymer fields:

$$G_0(\mathbf{x}_i - \mathbf{x}'_i; z_i) = \langle \psi_i^{a_i}(\mathbf{x}_i) \psi_i^{*a_i}(\mathbf{x}'_i) \rangle \cdot \tag{44}$$

It is now easy to show after a rescaling of the space variables $\mathbf{x}_i, \mathbf{x}'_i$, $i = 1, 2$, that the lattice size ξ is negligible if the polymer are sufficiently long. So it is possible to treat the discrete integrals in equation (43) as continuous ones. Going in the momentum space, the free correlation functions (44) become

$$\langle \tilde{\psi}_i^{a_i}(\mathbf{k}_i) \tilde{\psi}_i^{*a_i}(\mathbf{k}'_i) \rangle = \delta^{(3)}\left(\mathbf{k}_i - \mathbf{k}'_i\right) \frac{1}{\mathbf{k}_i^2 + m_i^2} \cdot \tag{45}$$

They are such that

$$G_0(\mathbf{x}_i - \mathbf{x}'_i; z_i) = \int \frac{\mathrm{d}^3 k}{(2\pi)^3} \mathrm{e}^{\mathrm{i}\mathbf{k}\cdot\mathbf{x}} \frac{1}{\mathbf{k}^2 + m_i^2}, \tag{46}$$

and

$$\begin{aligned} G_0(\mathbf{x}_i - \mathbf{x}'_i; L_i) &= \int_{c-\mathrm{i}\infty}^{c+\mathrm{i}\infty} \frac{M \mathrm{d}z_i}{2\pi\mathrm{i}} \mathrm{e}^{z_i L_i} G_0(\mathbf{x}_i - \mathbf{x}'_i; z_i) \\ &= \frac{1}{2} \left(\frac{M}{4\pi L_i} \right)^{3/2} \mathrm{e}^{-M(\mathbf{x}_i - \mathbf{x}'_i)^2/2L_i}. \end{aligned} \tag{47}$$

The partition function (22) is then given by the integral

$$\begin{aligned} Z = 2\pi \int \mathrm{d}^3 x_1 \mathrm{d}^3 x_2 \\ \times \lim_{\substack{\mathbf{x}'_1 \to \mathbf{x}_1 \\ \mathbf{x}'_2 \to \mathbf{x}_2}} G_0(\mathbf{x}_1 - \mathbf{x}'_1; L_1) G_0(\mathbf{x}_2 - \mathbf{x}'_2; L_2). \end{aligned} \tag{48}$$

The integrals at coinciding end points can easily be performed and we find

$$Z = \frac{2\pi M^3 V^2}{(4\pi)^3} (L_1 L_2)^{-3/2}. \tag{49}$$

It is important to realize that in equation (21), the limits of coinciding end points $\mathbf{x}'_i \to \mathbf{x}_i$ and the inverse Laplace transformations like that in (47) do *not* commute unless a proper renormalization scheme is chosen to eliminate the divergences caused by the insertion of the composite operators $|\psi^\alpha(\mathbf{x})|^2$. This can be seen for a single polymer. If we were to commuting the limit of coinciding end points with the Laplace transform, we would obtain

$$\int_{c-\mathrm{i}\infty}^{c+\mathrm{i}\infty} \frac{\mathrm{d}z}{2\pi} \mathrm{e}^{zL} \lim_{\mathbf{x}' \to \mathbf{x}} G_0(\mathbf{x} - \mathbf{x}'; z) = \int_{c-\mathrm{i}\infty}^{c+\mathrm{i}\infty} \frac{\mathrm{d}z}{2\pi\mathrm{i}} \mathrm{e}^{zL} G_0(\mathbf{0}, z), \tag{50}$$

where

$$G_0(\mathbf{0}; z) = \langle |\psi(\mathbf{x})|^2 \rangle \cdot \tag{51}$$

This expectation value, however, is linearly divergent:

$$\langle |\psi(\mathbf{x})|^2 \rangle = \int \frac{\mathrm{d}^3 k}{k^2 + m^2} \to \infty. \tag{52}$$

6 First Feynman diagram in Figure 2

At this point we start the computation of the numerator N of equation (41). From equation (41), the first diagram in Figure 2 corresponds to the following integral

$$\begin{aligned} N_1 = \frac{\kappa^2}{4} \lim_{\substack{n_1 \to 0 \\ n_2 \to 0}} \int_{c-\mathrm{i}\infty}^{c+\mathrm{i}\infty} \frac{M \mathrm{d}z_1}{2\pi\mathrm{i}} \frac{M \mathrm{d}z_2}{2\pi\mathrm{i}} \mathrm{e}^{z_1 L_1 + z_2 L_2} \\ \times \int \mathrm{d}^3 x_1 \mathrm{d}^3 x_2 \int \mathrm{d}^3 x'_1 \mathrm{d}^3 x'_2 \\ \times \left\langle |\psi_1^{a_1}(\mathbf{x}_1)|^2 |\psi_2^{a_2}(\mathbf{x}_2)|^2 \left(|\Psi_1|^2 \mathbf{A}_1^2\right)_{\mathbf{x}'_1} \left(|\Psi_2|^2 \mathbf{A}_2^2\right)_{\mathbf{x}'_2} \right\rangle \cdot \end{aligned} \tag{53}$$

which we are going to evaluate using the above lattice regularization with spacing given by the persistence length ξ. Replacing the expectation values by the Wick contractions corresponding to the first diagram in Figure 2, and performing the integrals as shown in the appendix, we obtain

$$\begin{aligned} N_1 = \frac{V}{4\pi} \frac{M^4}{(4\pi)^6} (L_1 L_2)^{-\frac{1}{2}} \int_0^1 \mathrm{d}s \left[(1-s)s\right]^{-\frac{3}{2}} \int \mathrm{d}^3 x \mathrm{e}^{-\frac{M\mathbf{x}^2}{2s(1-s)}} \\ \times \int_0^1 \mathrm{d}t \left[(1-t)t\right]^{-\frac{3}{2}} \int \mathrm{d}^3 y \mathrm{e}^{-\frac{M\mathbf{y}^2}{2t(1-t)}} \int \mathrm{d}^3 x''_1 \frac{1}{|\mathbf{x}''_1|^4} \cdot \end{aligned} \tag{54}$$

The variables $\mathbf{x}$ and $\mathbf{y}$, but not $\mathbf{x}''_1$, have been rescaled with respect to the original ones for later convenience. As a consequence, the lattices where $\mathbf{x}$ and $\mathbf{y}$ are defined have now spacings $\xi/\sqrt{L_1}$ and $\xi/\sqrt{L_2}$ respectively.

As we have already remarked, the chosen regularization is quite rigorous, but it makes difficult the evaluation of the integrals over the space variables in equation (54). Still, the $\mathbf{x}, \mathbf{y}$ integrals may be explicitly computed in the physically interesting limit $L_1, L_2 \gg \xi$, in which the above spacings become small and the discrete integrals can be replaced by usual integrals over continuous variables. At this point only the computation of

$$A(\xi) = \int \mathrm{d}^3 x''_1 \frac{1}{|\mathbf{x}''_1|^4} \tag{55}$$

remains to be done. $A(\xi)$ depends on the cut-off ξ, but not on the polymer lengths, so that it can be considered only as a numerical factor. Its analytical evaluation is still possible if one approximates the integral in $\mathbf{x}''_1$ with an integral over a continuous variable ρ and a cutoff in the ultraviolet region:

$$\int \mathrm{d}^3 x''_1 \frac{1}{|\mathbf{x}''_1|^4} \sim 4\pi^2 \int_\xi^\infty \frac{\mathrm{d}\rho}{\rho^2}. \tag{56}$$

After these approximations, we finally obtain

$$N_1 = V\pi^{1/2}\frac{M}{(4\pi)^3}(L_1L_2)^{-1/2}\xi^{-1}. \quad (57)$$

7 Second and third Feynman diagrams in Figure 2

Here we have to calculate

$$\begin{aligned} N_2 = \kappa^2 \lim_{\substack{n_1\to 0\\ n_2\to 0}} \int_{c-\mathrm{i}\infty}^{c+\mathrm{i}\infty} \frac{M\mathrm{d}z_1}{2\pi\mathrm{i}}\frac{M\mathrm{d}z_2}{2\pi\mathrm{i}}\mathrm{e}^{z_1L_1+z_2L_2} \\ \times \int \mathrm{d}^3x_1\mathrm{d}^3x_2 \int \mathrm{d}^3x_1'\mathrm{d}^3x_1''\mathrm{d}^3x_2' \\ \times \Big\langle |\psi_1^{a_1}(\mathbf{x}_1)|^2 |\psi_2^{a_2}(\mathbf{x}_2)|^2 \left(\mathbf{A}_1\cdot\Psi_1^*\boldsymbol{\nabla}\Psi_1\right)_{\mathbf{x}_1'} \\ \times \left(\mathbf{A}_1\cdot\Psi_1^*\boldsymbol{\nabla}\Psi_1\right)_{\mathbf{x}_1''} \left(\mathbf{A}_2^2\,|\Psi_2|^2\right)_{\mathbf{x}_2'} \Big\rangle . \end{aligned} \quad (58)$$

The above amplitude has no ultraviolet divergence, so that no regularization is required in principle. The Wick contractions pictured in the second Feynman diagrams of Figure 2 lead to the integral

$$N_2 = -4\sqrt{2}VL_2^{-1/2}L_1^{-1}\frac{M^3}{\pi^6}\int_0^1 \mathrm{d}t \int_0^t \mathrm{d}t' C(t,t'), \quad (59)$$

where $C(t,t')$ is a function independent of L_1 and L_2:

$$\begin{aligned} C(t,t') = [(1-t)t'(t-t')]^{-3/2} \\ \times \int \mathrm{d}^3x\mathrm{d}^3y\mathrm{d}^3z \mathrm{e}^{-M(\mathbf{y}-\mathbf{x})^2/2(1-t)} \\ \times \left(\nabla_{\mathbf{y}}^{\nu}\mathrm{e}^{-M\mathbf{y}^2/2t'}\right)\left(\nabla_{\mathbf{x}}^{\mu}\mathrm{e}^{-M\mathbf{x}^2/2(t-t')}\right) \\ \times \frac{\left[\delta_{\mu\nu}\mathbf{z}\cdot(\mathbf{z}+\mathbf{x}) - (z+x)_\mu z_\nu\right]}{|\mathbf{z}|^3|\mathbf{z}+\mathbf{x}|^3}. \end{aligned} \quad (60)$$

As in the previous section, the variables $\mathbf{x}, \mathbf{y}, \mathbf{z}$ have been rescaled with respect to the original ones in order to extract the behavior in L_1.

Again, if the polymer lengths are much larger than the persistence length one can ignore the fact that the monomers have a finite size and it is possible to compute $C(t,t')$ analytically, leading to

$$N_2 = -\frac{VL_2^{-1/2}L_1^{-1}}{(2\pi)^6}M^{3/2}4K, \quad (61)$$

where K is the constant

$$\begin{aligned} K \equiv \frac{1}{6}B\left(\frac{3}{2},\frac{1}{2}\right) + \frac{1}{2}B\left(\frac{5}{2},\frac{1}{2}\right) \\ -B\left(\frac{7}{2},\frac{1}{2}\right) + \frac{1}{3}B\left(\frac{9}{2},\frac{1}{2}\right) = \frac{19\pi}{384} \approx 0.154, \end{aligned} \quad (62)$$

and $B(a,b) = \Gamma(a)\Gamma(b)/\Gamma(a+b)$ is the Beta function. For large $L_1 \to \infty$, this diagram gives a negligible contribution with respect to N_1.

The third diagram in Figure 2 is the same as the second, except that L_1 and L_2 are interchanged.

$$N_3 = N_2|_{L_1\leftrightarrow L_2}. \quad (63)$$

8 Fourth Feynman diagram in Figure 2

Here we have the integral

$$\begin{aligned} N_4 = -4\kappa^2\frac{1}{2}\lim_{\substack{n_1\to 0\\ n_2\to 0}} \int_{c-\mathrm{i}\infty}^{c+\mathrm{i}\infty} \frac{\mathrm{d}z_1}{2\pi\mathrm{i}}\frac{\mathrm{d}z_2}{2\pi\mathrm{i}}\mathrm{e}^{z_1L_1+z_2L_2} \\ \times \int \mathrm{d}^3x_1\mathrm{d}^3x_2 \int \mathrm{d}^3x_1'\mathrm{d}^3x_2'\mathrm{d}^3x_1''\mathrm{d}^3x_2'' \\ \times \Big\langle |\psi_1^{a_1}(\mathbf{x}_1)|^2 |\psi_2(\mathbf{x}_2^{a_2})|^2 \left(\mathbf{A}_1\cdot\Psi_1^*\boldsymbol{\nabla}\Psi_1\right)_{\mathbf{x}_1'} \left(\mathbf{A}_1\cdot\Psi_1^*\boldsymbol{\nabla}\Psi_1\right)_{\mathbf{x}_1''} \\ \times \left(\mathbf{A}_2\cdot\Psi_2^*\boldsymbol{\nabla}\Psi_2\right)_{\mathbf{x}_2'} \left(\mathbf{A}_2\cdot\Psi_2^*\boldsymbol{\nabla}\Psi_2\right)_{\mathbf{x}_2''} \Big\rangle . \end{aligned} \quad (64)$$

which has no ultraviolet divergence. After some effort we find

$$\begin{aligned} N_4 = -\frac{1}{16}\frac{M^5V}{(2\pi)^{11}}(L_1L_2)^{-1/2} \\ \times \int_0^1 \mathrm{d}s \int_0^s \mathrm{d}s' \int_0^1 \mathrm{d}t \int_0^t \mathrm{d}t' C(s,s',t,t'), \end{aligned} \quad (65)$$

where

$$\begin{aligned} C(s,s';t,t') = [(1-s)s'(s-s')]^{-3/2}\,[(1-t)t'(t-t')]^{-3/2} \\ \times \int \frac{\mathrm{d}^3p}{(2\pi)^3}\left[\epsilon_{\mu\lambda\alpha}\frac{p^\alpha}{\mathbf{p}^2}\epsilon_{\nu\rho\beta}\frac{p^\beta}{\mathbf{p}^2} + \epsilon_{\mu\rho\alpha}\frac{p^\alpha}{\mathbf{p}^2}\epsilon_{\nu\lambda\beta}\frac{p^\beta}{\mathbf{p}^2}\right] \\ \times \Big[\int \mathrm{d}^3x'\mathrm{d}^3y' \mathrm{e}^{-\mathrm{i}\sqrt{L_1}\mathbf{p}(\mathbf{x}'-\mathbf{y}')}\mathrm{e}^{-M\mathbf{x}'^2/2(1-s)} \\ \times \left(\nabla_{\mathbf{y}'}^{\nu}\mathrm{e}^{-M\mathbf{y}'^2/2t'}\right)\left(\nabla_{\mathbf{x}'}^{\mu}\mathrm{e}^{-M(\mathbf{x}-\mathbf{y})^2/2(s-s')}\right)\Big] \\ \times \Big[\int \mathrm{d}^3u'\mathrm{d}^3v' \mathrm{e}^{-\mathrm{i}\sqrt{L_2}\mathbf{p}(\mathbf{u}'-\mathbf{v}')}\mathrm{e}^{-M\mathbf{v}'^2/2(1-t)} \\ \times \left(\nabla_{\mathbf{u}'}^{\rho}\mathrm{e}^{-M\mathbf{u}'^2/2t'}\right)\left(\nabla_{\mathbf{v}'}^{\lambda}\mathrm{e}^{-M(\mathbf{u}'-\mathbf{v}')^2/2(t-t')}\right)\Big], \end{aligned} \quad (66)$$

and $\mathbf{x}', \mathbf{y}'$ are scaled variables. To take into account the finite persistence length, they should be defined on a lattice with spacing $\xi/\sqrt{L_1}$. Similarly, $\mathbf{u}', \mathbf{v}'$ should be considered on a lattice with spacing $\xi/\sqrt{L_2}$. Without performing the space integrations $\mathrm{d}^3x'\mathrm{d}^3\mathbf{y}'\mathrm{d}^3\mathbf{u}'\mathrm{d}^3\mathbf{v}'$, the behavior of N_4 as a function of the polymer lengths can be easily estimated in the following limits:

1. $L_1 \gg 1; L_1 \gg L_2$

$$N_4 \propto L_1^{-1} \quad (67)$$

2. $L_2 \gg 1; L_2 \gg L_1$

$$N_4 \propto L_2^{-1} \quad (68)$$

3. $L_1, L_2 \gg 1, \quad L_2/L_1 = \alpha = \text{finite}$

$$N_4 \propto L_1^{-3/2}. \tag{69}$$

Moreover, if the lengths of the polymers are considerably larger than the persistence length, the function $C(s, s', t, t')$ can be computed in a closed form:

$$\begin{aligned} N_4 \approx & -\frac{128V}{\pi^5}\frac{M}{\pi^{3/2}}(L_1L_2)^{-1/2} \\ & \times \int_0^1 \mathrm{d}s \int_0^1 \mathrm{d}t(1-s)(1-t)(st)^{1/2} \\ & \times \left[L_1 t(1-s) + L_2(1-t)s\right]^{-1/2}. \end{aligned} \tag{70}$$

It is simple to check that this expression has exactly the above behaviors.

9 Final result

Collecting all contributions we obtain for the second topological moment:

$$\langle m^2 \rangle = \frac{N_1 + N_2 + N_3 + N_4}{Z}, \tag{71}$$

where N_1, N_2, N_3, N_4, Z are given by equations (53, 59, 65) and (48) respectively. This is an exact result, but to get an explicit expression of $\langle m^2 \rangle$ in the chosen lattice regularization, one is faced with the evaluation of discrete integrals which can be performed only numerically. However, polymers are in general very long flexible molecules, so that the limit $L_1, L_2 \gg \xi$ is of physical interest. In this case, the expressions of N_1, N_2, N_3, N_4, Z have been explicitly derived in equations (57, 61, 63, 70) and (49).

To discuss the physical content of the result (71), we consider a dilute solution containing n_p polymers $p_1, \ldots, p_{n_p}$ of lengths $l_1, \ldots, l_{n_p}$ respectively. Let $p_{\bar{k}}$ be a test polymer, whose topological relationships with respect to polymers $p_k, p_{k'}, \ldots$ etc. are given by the Gaussian linking numbers $m_{\bar{k}k}, m_{\bar{k}k'} \ldots$ etc. Clearly, it is licit to assume that, at least locally, the test polymer will not be able to distinguish this case from the situation in which it is winding up m times around another polymer of length $l_k + l_{k'} + \ldots$, where $m = m_{\bar{k}k} + m_{\bar{k}k'} + \ldots$ In the spirit of this approximation, we put $P_1 \equiv p_{\bar{k}}$ for the test polymer and replace the rest of the system with a long effective molecule P_2 of length $L_2 = \sum_{k \neq \bar{k}} l_k$. At this point we introduce the polymer concentration ρ as the average mass density of the polymers per unit volume:

$$\rho = \frac{\mathcal{M}}{V} \tag{72}$$

where $\mathcal{M}$ is the total mass of the polymers

$$\mathcal{M} = \sum_{k=1}^{N_p} \mu_a \frac{l_k}{a}. \tag{73}$$

Here μ_a is the mass of a single monomer of length a, thus l_k/a is the number of monomers in the polymer p_k. From the above relations we may write

$$L_2 \approx \frac{aV\rho}{\mu_a}. \tag{74}$$

In this way, the length of the effective molecule P_2 is expressed in terms of physical parameters, the concentration of polymers, the monomer length, and the mass and volume of the system. Inserting (74) into (71), with N_1, N_2, N_3, N_4, Z given by equations (49, 57, 61, 63), and (70). and keeping only the leading terms for $V \gg L_1^3$, we find for the average square winding number $\langle m^2 \rangle_{\mathrm{sol}}$ of the test polymers with all the other polymers in the solution the approximation

$$\langle m^2 \rangle \approx \frac{N_1 + N_2}{Z}, \tag{75}$$

Explicitly:

$$\langle m^2 \rangle_{\mathrm{sol}} \approx \frac{a\rho}{\mu_a}\left[\frac{\xi^{-1}L_1}{2\pi^{1/2}M^2} - \frac{2KL_1^{1/2}}{\pi^4 M^{3/2}}\right], \tag{76}$$

with K of (62). Since the persistence length is of the same order of the monomer length a and $M \sim a^{-1}$, $\langle m^2 \rangle_{\mathrm{sol}}$ is positive for large L_1 as it should.

10 Summary

We have set up a topological field theory to describe two fluctuating polymers P_1 and P_2 and calculated the second topological moment for the linking number m between P_1 and P_2. Since a finite number of diagrams and counterterms is involved in the computation, it is possible to derive an exact expression of the second topological moment using field theoretical techniques. This has been discussed in Section 4. To take into account also the finite monomer size, however, one is forced to consider the model on a lattice, with spacing given by the persistence length ξ. In this way, the contributions to $\langle m^2 \rangle$ given in equations (53, 59, 65) and (48) can be evaluated explicitly only numerically. Yet, we have seen that it is still possible to obtain an analytical result in the physical limit in which the polymers are sufficiently long.

As a physical application, it has been derived the square average number of intersections formed by a test polymer winding up around other polymers in a dilute solution. Our formula for $\langle m^2 \rangle_{\mathrm{sol}}$ of equation (76) is in agreement at the leading order in L_1 with an analogous formula computed in [5] without using field theories. Unfortunately, the method exploited in [5] is not able to estimate higher order corrections, while the above computations indicate that the nontrivial corrections should be suppressed by an inverse square root of the polymer lengths.

Of course, extreme care should be taken in applying equation (76) to real polymers. First of all, this result has

been obtained in the two-polymer approximation of [13]. Recently, the auxiliary configurational probability (4) has been generalized to treat an arbitrary number of polymers [17] and work is in progress in order to compute $\langle m^2\rangle_{\rm sol}$ with a better approximation. Even in that case, it always remains the limitation of using the Gauss linking number to distinguish the topological states of the system, which is common to all formulations of the statistical mechanics of polymers based on Edwards approach. Moreover, here the effects of the excluded volume interactions have been neglected. They will be the subject of forthcoming work.

Finally, let us emphasize the absence of infrared divergences in the topological field theory (11) in the limit of vanishing masses $m_1, m_2 = 0$. As a consequence, the second topological moment does not diverge in the limit of large L_1 if $\langle m^2\rangle$ is calculated from (11) for polymers passing through two fixed points $\mathbf{x}_1, \mathbf{x}_2$. This indicates a much stronger reduction of the configurational fluctuations by topological constraints than one might have anticipated.

Appendix

In this appendix we present the computations of the amplitudes $N_1, \ldots, N_4$. We shall need the following simple tensor formulas involving two completely antisymmetric tensors $\varepsilon^{\mu\nu\rho}$:

$$\varepsilon_{\mu\nu\rho}\varepsilon^{\mu\sigma\tau} = \delta^\sigma_\nu\delta^\tau_\rho - \delta^\tau_\nu\delta^\sigma_\rho, \quad \varepsilon_{\mu\nu\rho}\varepsilon^{\mu\nu\lambda} = 2\delta^\lambda_\rho. \tag{77}$$

The Feynman diagrams shown in Figure 2 corresponds to integrals over products of the polymer correlation functions G_0 defined in equation (52), which have to be integrated over space and Laplace transformed. For the latter we make use of the convolution property of the integral over two Laplace transforms $\tilde f(z)$ and $\tilde g(z)$ of the functions $f,\ g$:

$$\int_{c-\mathrm{i}\infty}^{c+\mathrm{i}\infty}\frac{M\mathrm{d}z}{2\pi\mathrm{i}}\mathrm{e}^{zL}\tilde f(z)\tilde g(z) = \int_0^L\frac{\mathrm{d}s}{M}f(s)g(L-s). \tag{78}$$

All spatial integrals are Gaussian of the form

$$\int \mathrm{d}^3x\mathrm{e}^{-a\mathbf{x}^2+2b\mathbf{x}\cdot\mathbf{y}} = (2\pi)^{3/2}a^{-3/2}\mathrm{e}^{b^2\mathbf{y}^2/a}, \quad a>0. \tag{79}$$

Contracting the fields in equation (53), and keeping only the contributions which do not vanish in the limit of zero replica indices, we find with the help of equations (77) and (78):

$$\begin{aligned} N_1 = &\int \mathrm{d}^3x_1,\mathrm{d}^3x_2\int_0^{L_1}\frac{\mathrm{d}s}{M}\int_0^{L_2}\frac{\mathrm{d}t}{M}\int \mathrm{d}^3x_1'\mathrm{d}^3x_2' \\ &\times G_0(\mathbf{x}_1-\mathbf{x}_1';s)G_0(\mathbf{x}_1'-\mathbf{x}_1;L_1-s)G_0(\mathbf{x}_2-\mathbf{x}_2';t) \\ &\times G_0(\mathbf{x}_2'-\mathbf{x}_2;L_2-t)\frac{1}{|\mathbf{x}_1'-\mathbf{x}_2'|^4}\cdot \end{aligned} \tag{80}$$

Performing the changes of variables

$$s' = \frac{s}{L_1},\ \ t' = \frac{t}{L_2},\ \ \mathbf{x} = \frac{\mathbf{x}_1-\mathbf{x}_1'}{\sqrt{L_1}},\ \ \mathbf{y} = \frac{\mathbf{x}_2-\mathbf{x}_2'}{\sqrt{L_2}}, \tag{81}$$

and setting $\mathbf{x}_1'' \equiv \mathbf{x}_1' - \mathbf{x}_2'$, we easily derive (54).

For small $\frac{\xi}{\sqrt{L_1}}$ and $\frac{\xi}{\sqrt{L_2}}$, we use the approximation (56). The space integrals can be done using the formula (79). After some work we obtain the result (68).

For the amplitude N_2 in equation (58) we obtain likewise the integral

$$\begin{aligned} N_2 = &\int \mathrm{d}^3x_1\mathrm{d}^3x_2\int \mathrm{d}^3x_1'\mathrm{d}^3x_1''\mathrm{d}^3x_2' \\ &\times\left[\int_0^{L_1}\frac{\mathrm{d}s}{M}\int_0^s\frac{\mathrm{d}s'}{M}G_0(\mathbf{x}_1'-\mathbf{x}_1;L_1-s)\right. \\ &\left.\times\,\nabla^\nu_{x_1''}G_0(\mathbf{x}_1-\mathbf{x}_1'';s')\nabla^\mu_{x_1'}G_0(\mathbf{x}_1''-\mathbf{x}_1';s-s')\right] \\ &\times D_{\mu\lambda}(\mathbf{x}_1'-\mathbf{x}_2)D_{\nu\lambda}(\mathbf{x}_1''-\mathbf{x}_2') \\ &\times\left[\int_0^{L_2}\frac{\mathrm{d}t}{M}G_0(\mathbf{x}_2-\mathbf{x}_2';L_2-t)G_0(\mathbf{x}_2'-\mathbf{x}_2;t)\right]. \end{aligned} \tag{82}$$

where $D_{\mu\nu}(\mathbf{x},\mathbf{x}')$ are the correlation functions (9–10) of the vector potentials. Setting $\mathbf{x}_2 \equiv \sqrt{L_2}\mathbf{u} + \mathbf{x}_2'$ and supposing that $\frac{\xi}{\sqrt{L_2}}$ is small, the integral over $\mathbf{u}$ can be easily evaluated with the help of the Gaussian integral (79). After the substitutions $\mathbf{x}_1'' = \sqrt{L_1}\mathbf{y} + \mathbf{x}_1$ $\mathbf{x}_1' = \sqrt{L_1}(\mathbf{y}-\mathbf{x}) + \mathbf{x}_1$, $\mathbf{x}_2' = \sqrt{L_1}(\mathbf{y}-\mathbf{x}-\mathbf{z}) + \mathbf{x}_1$ and a rescaling of the variables s, s' by a factor L_1^{-1}, we derive equation (59) with (60).

For small $\frac{\xi}{\sqrt{L_1}}, \frac{\xi}{\sqrt{L_2}}$, the spatial integrals are easily evaluated leading to:

$$\begin{aligned} N_2 = &\frac{-4VL_2^{-1/2}L_1^{-1}M^{3/2}}{(2\pi)^6} \\ &\times\int_0^1\mathrm{d}t\int_0^t\mathrm{d}t't'(1-t)\sqrt{\frac{t-t'}{1-t+t'}}\cdot \end{aligned} \tag{83}$$

After the change of variable $t' \to t'' = t - t'$, the double integral is reduced to a sum of integrals the type

$$c(n,m) = \int_0^1\mathrm{d}t\,t^m\int_0^t\mathrm{d}t't'^n\sqrt{\frac{t'}{1-t'}}, \quad m,n = \text{integers}.$$

These can be simplified by replacing t^m by $\mathrm{d}t^{m+1}/\mathrm{d}t(m+1)$, and doing the integrals by parts. In this way, we end up with a linear combination of integrals of the form:

$$\int_0^1\mathrm{d}t\frac{t^{\kappa+\frac{1}{2}}}{\sqrt{1-t}} = B\left(\kappa+\frac{3}{2},\frac{1}{2}\right). \tag{84}$$

The calculations of N_3 and N_4 are very similar, and may be omitted here.

References

1. S.F. Edwards, Proc. Phys. Soc. **91**, 51 (1967).
2. T.A. Vilgis, M. Otto, Phys. Rev. E **56**, R1314 (1997).
3. F. Tanaka, Prog. Theor. Phys. **68**, 148 (1982).
4. F. Tanaka, J. Phys. Soc. Jpn **53**, 2205 (1984).
5. M.G. Brereton, S. Shah, J. Phys. A **15**, 985 (1982).
6. D.J. Elderfield, J. Phys. A **15**, 1369 (1982).
7. H. Yamakawa, *Theory of Polymers Solutions* (Harper and Row, New York, 1971).
8. A.L. Kholodenko, T.A. Vilgis, Phys. Rep. **298**, 251 (1998).
9. S. Nechaev, *Statistics of Knots and Entangled Random Walks*, `cond-mat/9812105`.
10. H. Kleinert, *Path Integrals in Quantum Mechanics Statistics and Polymer Physics* (World Scientific, Singapore, 1995).
11. M.G. Brereton, T.A. Vilgis, J. Phys. A **28**, 1149 (1995).
12. M. Otto, T.A. Vilgis, Phys. Rev. Lett. **80**, 881 (1998).
13. M.G. Brereton, S. Shah, J. Phys. A **13**, 2751 (1980).
14. F. Ferrari, I. Lazzizzera, Nucl. Phys. B **559**, 673 (1999).
15. M. Chaichian, W.F. Chen, *Phys. Rev.* D **58**, 5004 (1998).
16. E. Guadagnini, M. Martellini, M. Mintchev, Nucl. Phys. B **336**, 581 (1990); J.M.F. Labastida, A.V. Ramallo, Phys. Lett. B **238**, 214 (1989).
17. F. Ferrari, H. Kleinert, I. Lazzizzera, *Field Theory of N Entangled Polymers*, to appear in Int. J. Mod. Phys. B, `cond-mat/0005300`.